Applied Analysis and Optimization
Volume 6, Number 2, 2022, 313–328

Yokohama Publishers
ISSN 2189-1664 Online Journal

VISCOUS SPLITTING FINITE DIFFERENCE SCHEMES TO CONVECTION-DIFFUSION EQUATIONS WITH DISCONTINUOUS COEFFICIENT

HARI MOHAN SRIVASTAVA, MOHAMMAD IZADI, AND NASRIN OKHOVATI

Abstract. In this research paper, we utilize the splitting finite difference methods to obtain the numerical solutions of one dimensional convection-diffusion equations with a discontinuous convective flux function. Based on operator splitting, the underlying equation is split into two successive initial value problems consisting of a pure convection equation and a pure diffusion equation. While the solution algorithms for the convection part involve an upwind immersed interface scheme and a two-stage conservative finite difference approximation, for the diffusion part three popular unconditionally stable methods are employed. The computational accuracy of the proposed combined methods is studies Numerical experiments using both linear and non-linear model problems indicate that the presented methods capable of providing stable as well as accurate solutions.

1. Introduction

Several realistic practical problems in science and engineering such as Euler equations arising in gas dynamics, equations of motions, continuity, energy, and etc. can be described by a conservation law equation

$$\frac{\partial u}{\partial t} + \frac{\partial}{\partial x} F(u) = 0. \tag{1.1}$$

These kinds of problems have been considered in many research agendas over the years both from a mathematical, physical, and numerical point of view (see [21]). The function $F(u)$ in (1.1) is the so-called flux function, which is a smooth function in general for hyperbolic conservation laws. When dealing with these types of equations, several numerical troubles are to be expected. Among other difficulties, let us mention the approximation of sharp front, shock wave, etc. It is well-known that even for a smooth initial condition, the hyperbolic conservation laws (1.1) does not always have a solution in the classical sense. Instead, solutions defined based on concept of distributions must be considered. These solutions are called weak solutions. These weak solutions turn out to be nonunique and therefore an extra condition, i.e., entropy criteria is introduced to characterize the physically relevant solution (see [21]). However, the flux function may have a discontinuity through the spatial variable. As a simple realistic physical model problem that describes a conservation law having discontinuous flux function, one may mention the Witham model of car traffic flow on a highway (see [21]). Conservation laws having discontinuous flux function in x appears in an increasing number of problems

2020 *Mathematics Subject Classification.* 65M06, 65F30, 76M20, 34A36.
Key words and phrases. Discontinuous flux; finite difference approximation; operator splitting; MacCormack scheme; upwind method.

due to their wide range of applications. Among others, in the modelling of two phase flow in a porous media (see [7]), in sedimentation problem (see [5], [6] and [2]) and in traffic jam on roads with varying conditions (see [23] and [9]).

This study presents a number of finite difference approximations based on operator splitting to treat convection-diffusion equations as a generalization of (1.1) in one spatial dimension with discontinuous convective term. To be more precise, we consider

$$\begin{cases} \frac{\partial u}{\partial t} + \frac{\partial}{\partial x} F(u, \gamma(x)) & = \epsilon \frac{\partial^2 u}{\partial x^2}, \quad (x,t) \in \Omega := \mathbb{R} \times \mathbb{R}^+, \\ u(x,0) & = u_0(x), \quad x \in \mathbb{R}, \end{cases} \tag{1.2}$$

In (1.2), $u = u(x,t)$ denotes the scalar unknown function to be found, $u_0 : \mathbb{R} \longrightarrow \mathbb{R}$ is a known function, and ϵ is a small non-negative constant. The flux $F(u, \gamma(x))$ in (1.2) has a possibly discontinuous spatial dependence through the coefficient $\gamma(x)$. The function $\gamma(x)$ is supposed to be a piecewise smooth function having a finite number of jump discontinuities. Below, for simplicity, we also assumed that $\gamma(x)$ has only one point of discontinuity which is located at $x = 0$. This make the line $x = 0$ an interface for our problem. A typical example of such flux functions that we will particularly consider has the following multiplicative form

$$F(u, \gamma(x)) = \gamma(x) f(u), \quad \gamma(x) = \begin{cases} \gamma^-, & x < 0, \\ \gamma^+, & x > 0, \end{cases} \tag{1.3}$$

being f is a smooth function and γ^-, γ^+ are two non-zero constants. Indeed, equation (1.2) is a particular case of the following model problem, which is a non-linear degenerate convection-diffusion of parabolic type

$$\frac{\partial u}{\partial t} + \frac{\partial}{\partial x} F(u, \gamma(x)) = \frac{\partial^2}{\partial x^2} A(u), \tag{1.4}$$

where A is a given function. The authors in [18] constructed approximate solutions based on an upwind finite difference approach of Engquist-Osher type for this kind of problems. Let we utilize the linear flux function $f(u) = u$ and $\epsilon = 0$ in (1.3). In this respect, an immersed upwind interface method was introduced in [34] to construct the interface criteria into the numerical flux. In contrast to the upwind schemes that are only first-order accurate, the authors in [26] proposed the second-order MacCormack method, which is an explicit conservative finite difference scheme to treat (1.2) numerically. Moreover, the Rung-Kutta discontinuous Galerkin method for closely related problem was developed in [25]. Moreover, some other approximate methods have been developed for the closely related model problems to (1.3) can be found in [10] to [30] and in [3,24,29,32,35–37]. For an overview of some mathematical results devoted to the problem (1.4) we refer the interested reader to [18] and [19] and also to the references therein.

In this manuscript, we are interested in developing a number of simple computational procedures for (1.2) when the convective flux (1.3) is utilized. It is well-known that classical finite difference approaches present nonphysical oscillations for model problems with sharp front and in particular with discontinuous coefficients. The main focus is to investigate the applicability of the operator splitting strategies for the convection-diffusion problems that have a discontinuous coefficient. The

principle idea of several successful computational approaches for treating equations such as (1.2), is based on viscous operator splitting strategy. This implies that we splits the time evolution into two subproblems to separate the impacts of diffusion (viscosity) and convection. For instance, in [4] the accuracy, stability, as well as the convergence properties of the basic operator splitting schemes are investigated when these schemes are utilized to calculate discontinuous solutions of hyperbolic scalar conservation laws (1.1) in two dimensions. In particular, they proved that the Strang splitting procedure and the first-order splitting method always converge to the unique weak solution, which satisfies the entropy criteria. The paper [17] presents a semi-discrete scheme to find the approximate solutions of convection-diffusion equation in m dimensional. The proposed algorithm is relied on the utilization of operator splitting to separate the diffusion part and the convection part of the underlying equation.

The remaining of this study is organised as follows. Section 2 is devoted to present some notations that will be used in the subsequent sections. Then, we concisely describe the main ideas of operator splitting techniques for solving the time-dependent model problems of convection-diffusion types by decomposing them into a nonlinear and linear subproblems. This consists of introducing two popular splitting schemes i.e., sequential and Strang splitting strategies, which are shortly illustrated from the viewpoint of the local splitting errors. Hence, we develop various numerical techniques to approximate the solutions of nonlinear and linear subproblems individually such that by combining them the solution of the original equation (1.3) is constructed. These schemes are then tested on a linear as well as non-linear example in Section 3. We also justify the first and second-order accuracy of the proposed methods throughout the course of numerical simulations. The manuscript ends with some conclusions in Section 4.

2. Finite difference approximations

Firstly, we introduce some terminologies and notations to construct the finite difference methods. Throughout this paper, for the numerical schemes, the time step and spatial step size are denoted by Δx and Δt respectively. Let assume that the spatial domain $\mathbb{R}$ is partitioned into the elements $I_j = [x_{j-\frac{1}{2}}, x_{j+\frac{1}{2}})$ with grid points $x_{j-\frac{1}{2}} = j\Delta x$, $j \in \mathbb{Z}$. Here, $\Delta x = x_{j+\frac{1}{2}} - x_{j-\frac{1}{2}}$ is the mesh size. We will also set the midpoints of the intervals as $x_j = \frac{1}{2}(x_{j-\frac{1}{2}} + x_{j+\frac{1}{2}}), \forall j \in \mathbb{Z}$. In the same manner, we will divide the time domain $\mathbb{R}^+$ into $I_n = [t_n, t_{n+1})$, where $t_n = n\Delta t$ for $n \in \mathbb{N} \cup \{0\}$, and $\Delta t = t_{n+1} - t_n$ denotes the uniform time step. On the computational grid (x_j, t_n) we use U_j^n to denote the numerical solution derived via finite difference approach for to the exact solution $u(x_j, t_n)$ of (1.2). We will also set

$$\mu = \frac{\Delta t}{\Delta x}, \quad \mathcal{I}(u, v) = \Big[\min\{u, v\}, \max\{u, v\}\Big], \quad \mu^{\pm} = \gamma^{\pm}\frac{\Delta t}{\Delta x}.$$

Finally, let us discretize the initial condition $u_0(x)$. The initial condition $u_0(x)$ is considered as follows

$$U_j^0 = \frac{1}{\Delta x}\int_{I_j} u_0(x)dx, \quad \forall j \in \mathbb{Z},$$

which means that the initial data is projected into the space of piecewise constant functions.

2.1. **Splitting methods.** The main idea of operator splitting technique is to convert the solution of an initial value problem into to the solution of some simpler model problems. For the nonlinear equations, this task is to decompose a problem into nonlinear and linear subproblems. Hence, we require to solve each subproblem separately for small temporal steps Δt, and then concatenate the solutions at the end of each time step. To introduce the main ideas of operator splitting methods, let us first rewrite (1.2) as follows

$$\frac{\partial}{\partial t}u(x,t) = (\mathcal{L}+\mathcal{N})\,u(x,t). \tag{2.1}$$

Here, the nonlinear operator $\mathcal{N}$ as well as the linear operator $\mathcal{L}$ are defined respectively as

$$\mathcal{N} := -\frac{\partial}{\partial x}F(\cdot,\gamma(x)), \quad \mathcal{L} := \epsilon\frac{\partial^2}{\partial x^2}.$$

To proceed, we require to approximate the exact solution of (1.2) by solving two linear and nonlinear subproblems. Let assume that $S_N(t)$ and $L_N(t)$ denote the exact solution operators of the related diffusive and convective subproblems

$$\tfrac{\partial}{\partial t}w(x,t) = \mathcal{L}(w), \quad w(x,0) = w_0(x), \tag{2.2a}$$

$$\tfrac{\partial}{\partial t}v(x,t) = \mathcal{N}(v), \quad v(x,0) = v_0(x), \tag{2.2b}$$

in a given sequential order. Let us denoted $u(x,t) \equiv S(t)u_0$ to be the unique weak solution of (1.2), which satisfies the entropy conditions. Analogously, let $v(x,t) \equiv S_N(t)v_0$ and $w(x,t) \equiv S_L(t)w_0$ denote the (weak) solutions satisfying the one-dimensional problems (2.2a)-(2.2b).

In this work, we are mainly aimed at the first as well as the second order operator splitting methods. The evolution of time in the first-order operator splitting method consists of two steps that abstractly can be expressed as

$$S(T)u_0 = \Big(S_N(\Delta t)\circ S_L(\Delta t)\Big)^n u_0 \qquad (n\Delta t = T). \tag{2.3}$$

This is called sequential or Godunov's fractional splitting method (see [8]). We note that the order in (2.3) can also be reversed

$$S(T)u_0 = \Big(S_L(\Delta t)\circ S_N(\Delta t)\Big)^n u_0 \qquad (n\Delta t = T).$$

It should be noted that it is not yet known which ordering leads to better performance in the literature. Now, each subproblems can be discretized independently using different methods.

In the second-order operator splitting methods, the advancement in time is performed in three steps. This particular splitting procedure is also known as the standard *Strang* splitting. In this version, the solution takes the following form:

$$S(T)u_0 = \left(S_N\Big(\frac{\Delta t}{2}\Big)\circ S_L(\Delta t)\circ S_N\Big(\frac{\Delta t}{2}\Big)\right)^n u_0 \qquad (n\Delta t = T) \tag{2.4}$$

or

$$S(T)u_0 = \left(S_L\Big(\frac{\Delta t}{2}\Big) \circ S_N(\Delta t) \circ S_L\Big(\frac{\Delta t}{2}\Big) \right)^n u_0 \qquad (n\Delta t = T).$$

In this respect, in the scheme (2.4), as a first step, we solve (2.2a) using the initial condition of the original problem, and then, utilize the obtained solution as an initial condition to solve (2.2b), at last utilize the solution as the initial condition, solve (2.2a) and derive the numerical solution.

It is theoretically proven (see [20] and [31]) that the second-order accuracy of the method (2.4) is guaranteed when the two parts are solved with at least second-order accuracy. In this study, we solve the nonlinear subequation (2.2a) by using the MacCormack scheme, which is a second-order scheme. Thus, to achieve a second-order accuracy with (2.4) we require that the linear subequation (2.2b) is solved by a second-order method. For this purpose, we will use three popular schemes such as MacCormack, Crank-Nicolson, and alternating direction explicit method for solving the linear counterpart. However, for comparison purpose, we will also utilize the first-order upwind scheme for (2.2a) and simple first-order methods like FTCS (forward in time and central in space) for the diffusion problem, which may only be first-order in time. Clearly, in this case one achieves only the first-order accuracy in time and our splitting will be based upon the first-order version (2.3). In the following subsections we will illustrate these numerical procedure in more details.

2.2. **Methods for the nonlinear convection equation.** We are going to illustrate the schemes that we utilize to approximate the nonlinear convective subproblem (2.2a). We first develop an upwind scheme and then utilize this scheme to devise a second-order numerical scheme for (2.2a). The first-order upwind scheme plays an fundamental role in the development of second-order MacCormack scheme below. In fact, upwind procedure uses concepts from characteristic theory to specify the direction of spatial differencing.

I) Upwind scheme. To proceed, let we are given two (two-point) numerical flux functions $\mathcal{F}^{\pm} : \mathbb{R}^2 \longrightarrow \mathbb{R}$, which are locally Lipschitz continuous and satisfy the consistency property $\mathcal{F}^{\pm}(v, v) = \gamma^{\pm} f(v)$. Given V_j^n at the time level t_n, we calculate the discrete V_j^{n+1} via the following three-point numerical scheme

$$V_{j-1}^{n+1} = V_{j-1}^n - \mu(\mathcal{F}_j^{n,-} - \mathcal{F}_{j-1}^{n,-}) \qquad (j \leqq 0;\ n \geqq 0), \tag{2.5a}$$

$$V_j^{n+1} = V_j^n - \mu(\mathcal{F}_{j+1}^{n,+} - \mathcal{F}_j^{n,+}) \qquad (j \geqq 0;\ n \geqq 0), \tag{2.5b}$$

where $\mathcal{F}_j^{n,\pm} = \mathcal{F}^{\pm}(V_{j-1}^n, V_j^n)$. Note that the coupling of two finite difference schemes (2.5a) and (2.5b) is carried out by evaluating $\mathcal{F}_0^{n,\pm} = \mathcal{F}^{\pm}(V_{-1}^n, V_0^n)$. To complete the definition of the scheme we require to specify the numerical flux functions $\mathcal{F}^{\pm}$. Far from the interface, we utilize the standard upwind flux. This implies that for $j \neq 0$, the computation of $\mathcal{F}_j^{n,\pm}$ is done by

$$\mathcal{F}^{\pm}(v, w) = \begin{cases} f^{\pm}(v), & \text{if } \dot{S} \geq 0, \\ f^{\pm}(w), & \text{if } \dot{S} < 0, \end{cases} \quad \dot{S} = \begin{cases} \frac{f^{\pm}(w) - f^{\pm}(v)}{w - v}, & \text{if } v \neq w, \\ (f^{\pm})'(v), & \text{if } v = w, \end{cases} \tag{2.6}$$

where we have used $f^{\pm}(v) = \gamma^{\pm} f(v)$. In order to define the numerical coupling procedure, one needs to specify both fluxes $\mathcal{F}_0^{n,-}$ and $\mathcal{F}_0^{n,+}$ more precisely. For this purpose, depending on the sign of the derivative of $f^{\pm}$ the following cases are considered:

a) $(f^{\pm})'(u) > 0$, for all $u \in \mathcal{I}(V_j^n, V_{j+1}^n)$,
b) $(f^{\pm})'(u) < 0$, $\alpha = L, R$, for all $u \in \mathcal{I}(V_j^n, V_{j+1}^n)$,
c) $(f^{-})'(u) > 0$ and $(f^{+})'(u) < 0$ for all $u \in \mathcal{I}(U_j^n, V_{j+1}^n)$.

In the first case a) we only need to determine $\mathcal{F}_0^{n,+}$ that takes the form

$$\mathcal{F}_0^{n,+} = f^{-}(V_{-1}^n). \tag{2.7a}$$

For instance, in the case of linear flux $f^{\pm}(v) = \gamma^{\pm} v$ with $\gamma^{\pm} > 0$, the numerical scheme (2.5) can be rewritten as

$$\begin{cases} V_j^{n+1} = (1-\mu^{-})V_j^n + \mu^{-} V_{j-1}^n, & \text{if } j \leqq -1, \\ V_j^{n+1} = (1-\mu^{-})V_j^n + \mu^{+} V_{j-1}^n, & \text{if } j = 0, \\ V_j^{n+1} = (1-\mu^{+})V_j^n + \mu^{+} V_{j-1}^n, & \text{if } j \geqq 1. \end{cases}$$

The parameters $\mu^{\pm}$ are called the Courant-Friedrichs-Lewy numbers or CFL numbers. The CFL plays an essential role in determining the stability of a numerical scheme. Standard stability analysis dictates that these CFL numbers should be chosen such that $0 < \mu^{\pm} < 1$. In the second case b) it is sufficient to take $\mathcal{F}_0^{n,-}$ as

$$\mathcal{F}_0^{n,-} = f^{+}(V_0^n). \tag{2.7b}$$

Again, utilizing the linear flux $f^{\pm}(v) = \gamma^{\pm} v$ with $\gamma^{\pm} < 0$ in (2.5) after a rearrangement one gets

$$\begin{cases} V_j^{n+1} = (1+\mu^{-})V_j^n - \mu^{-} V_{j+1}^n, & \text{if } j \leqq -2, \\ V_j^{n+1} = (1+\mu^{-})V_j^n - \mu^{+} V_{j+1}^n, & \text{if } j = -1, \\ V_j^{n+1} = (1+\mu^{+})V_j^n - \mu^{+} V_{j+1}^n, & \text{if } j \geqq 0. \end{cases}$$

In the third and last case c), we consider fluxes that have opposite signs. In this situation no extra requirement like (2.7a) or (2.7b) is needed for numerical treatment of the interface and the numerical flux defined in (2.6) is sufficient for computing V_{-1}^{n+1} and V_0^{n+1}. If we consider the linear flux with $\gamma^{-} > 0$ and $\gamma^{+} < 0$ as in the two former cases, we get

$$\begin{cases} V_j^{n+1} = (1-\mu^{-})V_j^n + \mu^{-} V_{j-1}^n, & \text{if } j \leqq -1, \\ V_j^{n+1} = (1+\mu^{+})V_j^n - \mu^{+} V_{j+1}^n, & \text{if } j \geqq 0. \end{cases}$$

II) MacCormack scheme. The upwind scheme already illustrated in the last section, has at most first-order accuracy. This yields to poor accuracy for model problems with nonsmooth data. To alleviate these difficulties, we utilize the idea of MacCormack [22] to formally upgrade the upwind scheme (2.5) to second-order accuracy. This new scheme are obtained by correcting first-order schemes.

The standard algorithm based on MacCormack original scheme consists of a two-stage procedure known as the predictor-corrector method. This explicit scheme can

be presented for the (classical) conservation laws (1.1) as follows

$$\text{Predictor step}: \; V_j^\star = V_j^n - \mu\,\Delta_x^+ F_j^n, \tag{2.8a}$$

$$\text{Corrector step}: \; V_j^{\star\star} = V_j^n - \mu\,\Delta_x^- F_j^{n,\star}. \tag{2.8b}$$

Here, the backward and forward difference operators Δ_x^-, Δ_x^+ are defined as

$$\Delta_x^- V_j = V_j - V_{j-1}, \quad \Delta_x^+ V_j = V_{j+1} - V_j.$$

Here, F_j^n and $F_j^{n,\star}$ are denoted by the flux F evaluated at V_j^n and $V_j^\star$ respectively. Hence, the solution V_j^{n+1} at the next time step becomes

$$V_j^{n+1} = \frac{1}{2}(V_j^\star + V_j^{\star\star}). \tag{2.8c}$$

It should be stressed that, the first-order spatial derivatives in (2.8a)-(2.8b) are discretized with opposite one-sided finite differences in the corrector and predictor stages. The forward differencing operator is utilized in the predictor stage and backward differencing operator is utilized in the corrector stage. However, applying these operators in the stages may be interchanged depending on the flux F as we see in the case of our model problem.

To express the MacCormack scheme in a conservative form and suitable for (1.2), we take the numerical fluxes $\mathcal{H}_\pm$ as

$$\mathcal{H}_\pm(u, v) = \frac{1}{2}\Big(f^\pm(u) + f^\pm(v)\Big). \tag{2.9}$$

In fact, by putting (2.8a) into (2.8b) followed by inserting the obtained result into (2.8c) it can be written as conservative. Obtaining the predicted numerical values $V_j^\star$ at the first stage by the upwind scheme (2.5), the corrected numerical values V_j^{n+1} at the next time level is given by

$$V_{j-1}^{n+1} = V_{j-1}^n - \mu\,\Delta_x^\pm \mathcal{H}_{j,-}^{n,\star} \qquad (j \leqq 0;\; n \geqq 0), \tag{2.10a}$$

$$V_j^{n+1} = V_j^n - \mu\,\Delta_x^\pm \mathcal{H}_{j,+}^{n,\star} \qquad (j \geqq 0;\; n \geqq 0), \tag{2.10b}$$

where

$$\mathcal{H}_{j,\pm}^{n,\star} = \mathcal{H}_\pm(V_{j-1}^n, V_j^\star),$$

and $\Delta_x^\pm$ denotes either the forward or backward difference operator. As mentioned before, if for computing $V_j^\star$ in the range $j \leqq 0$ ($j \geqq 0$), one uses Δ_x^- or Δ_x^+, which completely depends on $f^\pm$, then in (2.10) we require to utilize an difference one-sided operation that has the opposite sign. Utilizing both backward and forward differences for space derivatives in computing the average value of the time derivative in (2.8c) is the main reason for second-order accuracy. As an illustration, consider the linear flux functions $f^\pm(v) = \gamma^\pm v$ with $\gamma^- > 0$ and $\gamma^+ < 0$. Thus, the numerical schemes (2.8a)-(2.8b) will be reduced to

$$\begin{cases} V_j^{n+1} = V_j^n - \mu^-\,\Delta_x^+ V_j^\star, \quad V_j^\star = V_j^n - \mu^-\,\Delta_x^- V_j^n, & \text{if } j \leqq -1, \\ V_j^{n+1} = V_j^n - \mu^+\,\Delta_x^- V_j^\star, \quad V_j^\star = V_j^n - \mu^+\,\Delta_x^+ V_j^n, & \text{if } j \geqq 0. \end{cases}$$

2.3. **Methods to treat the linear diffusion equation numerically.** To solve the linear diffusion equation (2.2b) several numerical procedures may be applied. Let W_j^n denotes the numerical solution calculated at the time level t_n. Among others, the following schemes are considered in this work:

A) Laasonen method or forward in time and implicit central in space (FTICS):.

$$-r\,W_{j-1}^{n+1} + \big(1+2r\big)W_j^{n+1} - r\,W_{j+1}^{n+1} = W_j^n.$$

This is an implicit prcedure with truncation error $\mathcal{O}(\Delta t + \Delta x^2)$, which means that it is first-order accurate. Moreover, it is unconditionally stable scheme (see [33]).

B) Crank-Nicolson (CN) method:

$$-\frac{r}{2}\,W_{j-1}^{n+1} + \big(1+r\big)W_j^{n+1} - \frac{r}{2}\,W_{j+1}^{n+1} = -\frac{r}{2}\,W_{j-1}^{n} + \big(1-r\big)W_j^{n} - \frac{r}{2}\,W_{j+1}^{n}.$$

This is an implicit method and has second-order accuracy. It can be show that the truncation error $\mathcal{O}(\Delta t^2 + \Delta x^2)$, and unconditionally stable scheme (see [33]). It should be note that when using the two above schemes for solving the diffusion equation, in each time step the solution procedure involves only solving tridiagonal matrices. Next, we introduce a seemingly implicit scheme that has not such property and indeed is an explicit method.

C) Alternating-directional explicit (ADE) methods: The left to right (L→R) as well as the right to left (R→L) numerical schemes for the diffuion equation (2.2b) due to Saulyev (see [27] and [28]) are, respectively, defined as follows:

$$\big(1+r\big)\,W_j^{n+1} = r\,W_{j-1}^{n+1} + \big(1-r\big)\,W_j^n + r\,W_{j+1}^n, \tag{2.11a}$$

$$\big(1+r\big)\,W_j^{n+1} = r\,W_{j+1}^{n+1} + \big(1-r\big)\,W_j^n + r\,W_{j-1}^n. \tag{2.11b}$$

We emphasize that both the R→L and L→R formulae are seemingly implicit in nature but can be solved in an explicit manner from left (right) to right (left) using the imposed boundary condition on the left (right) to get started. Based upon the L→R and R→L approximations, the first ADE scheme was proposed by Saulyev as follows (see [28]):

$$\big(1+r\big)\,W_j^{n+1} = r\,W_{j-1}^{n+1} + \big(1-r\big)\,W_j^n + r\,W_{j+1}^n, \tag{2.12a}$$

$$\big(1+r\big)\,W_j^{n+2} = r\,W_{j+1}^{n+2} + \big(1-r\big)\,W_j^{n+1} + r\,W_{j-1}^{n+1}. \tag{2.12b}$$

The aforementioned scheme has second-order accuracy with $\mathcal{O}(\Delta t^2+\Delta x^2+\Delta t^2/\Delta x^2)$ as the truncation error. Also it is an unconditionally stable scheme. Note that if r is constant, the scheme is formally first-order because of the presence of the inconsistent term $\mathcal{O}(\Delta t/\Delta x)^2$. To get ride of this inconsistence term, the second ADE version is proposed in [1], in which the computations are performed simultaneously in both R→L and L→R directions and the resulting solutions are averaged to obtain the ultimate $W_j^{n+1} = \frac{1}{2}\left(p_j^{n+1} + q_j^{n+1}\right)$:

$$\big(1+r\big)\,p_j^{n+1} = r\,p_{j-1}^{n+1} + \big(1-r\big)\,p_j^n + r\,p_{j+1}^n, \tag{2.13a}$$

$$\big(1+r\big)\,q_j^{n+1} = r\,q_{j+1}^{n+1} + \big(1-r\big)\,q_j^n + r\,p_{j-1}^{n+1}. \tag{2.13b}$$

This scheme is also unconditionally stable. Also, its truncation error is $\mathcal{O}(\Delta t^2 + \Delta x^2)$. In fact, when averaging is used the term $\mathcal{O}(\Delta t/\Delta x)^2$ cancel out an the resulting method becomes second-order.

To summarize, we consider the performance of the following schemes as combinations of previously proposed numerical methods applied to the linear and nonlinear subproblems (2.2a) and (2.2b) respectively:

- Upwind and ADE/CN/FTCS: Upwind-ADE/CN/FTCS,
- MacCormack and ADE/CN/MacCormack: Mac-ADE/CN/Mac.

For comparison purposes, the methods upwind (see [34] and [26] and MacCormack [26] are also considered in the numerical experiments below.

3. Experimental results

Let us investigate the performance of the MacCormack scheme applied to problem (1.2). In this respect, several numerical simulations are carried out using both linear as well as nonlinear model problems. The computational domain is taken as $[-1, 1]$ and the final time is $t = T$ in terms of second. We partition the given domain $[-1, 1]$ into M subintervals with uniform mesh size Δx and using $M = 2^s, s = 4, 5, \cdots, 10$. We further divided $[0, T]$ into $N = \lceil \frac{T}{\Delta t} \rceil$ time steps. To check the accuracy of the presented combined methods, the relative L_1, L_2 and L_∞ error between the exact true solution u_e and the numerical counterpart $U_{\Delta x}$ are given with following definitions

$$E(\Delta x, p) = \|U_{\Delta x} - u_e\|_p \qquad (p = 1, 2, \infty).$$

Also, the rate of convergence is calculated using the formula

$$\log_2 \left(\frac{E(\Delta x, p)}{E(\Delta x/2, p)} \right)$$

for $p = 1, 2$ and $p = \infty$.

3.1. **Linear case.**

To deal with linear model problems, we take the linear flux function as $f^{\pm}(u) = \gamma^{\pm} u$. Using Fourier stability analysis it is not a difficult task to show that applying the upwind and MacCormack schemes to $\partial_t u + \partial_x f^{\pm}(u) = 0$ is stable under the following condition

$$0 < \max\{|\gamma^-|, |\gamma^+|\} \cdot \mu < 1.$$

Therefore, to guarantee the stability of the schemes the time step Δt is taken to be sufficiently small. In the linear case, the final time $T = 0.1$ and $T = 0.5$ are used for the computations.

Example 3.1. We first study the model problem (1.2) with $\gamma^- = 0.02$ and $\gamma^+ = -0.04$ and take the initial condition for $u_0(x)$ defined as follows:

$$u(x, 0) = \begin{cases} 1, & |x| \leqq \frac{1}{4}, \\ \frac{1}{2}, & \frac{1}{4} < |x| \leqq \frac{3}{4}. \\ 0, & \text{otherwise.} \end{cases}$$

Obviously, $u_0(x)$ is discontinuous at $\pm\frac{1}{4}, \pm\frac{3}{4}$. This example is considered in [26].

The numerical outcomes for this test problem are summarized in Tables 1-2 and also in Figs. 1-2. In these experiments, diverse values of Δx and Δt and final time T. The viscosity is set $\epsilon = 0.001$. In Table 1, we present the numerical results calculated at $T = 0.1$ derived by the sequential splitting procedure (2.3) using $\Delta t = 0.001$ for a different choices of the number of spatial grid points $M = 25, 50, 100$, and 200. In the aforementioned Table, the performance of various schemes including Upwind-ADE/CN/FTCS and Mac-ADE/CN/Mac are reported in the L_1 norm. Note that, our experiments show that the corresponding results obtained based on the Strang splitting procedure (2.4) are almost the same as the results of the sequential splitting and therefore we omit them. Note that in the ADE we utilize the second version (2.13a)-(2.13b) which is based on the averaging.

TABLE 1. Comparison of L_1 error norms for different finite difference schemes based on sequential splitting for Example 3.1 with $\Delta t = 0.001$, $\epsilon = 0.001$, and $\Delta x = 0.08, 0.04, 0.02, 0.01$ evaluated at time $T = 0.1$.

Method	$M = 25$	$M = 50$	$M = 100$	$M = 200$
Upwind [27]	1.6463E-2	1.1872E-2	4.1279E-3	1.8396E-3
Upwind-ADE	1.6462E-2	1.1867E-2	4.1340E-3	1.8236E-3
Upwind-CN	1.6462E-2	1.1867E-2	4.1340E-3	1.8239E-3
Upwind-FTCS	1.6462E-2	1.1864E-2	4.1364E-3	1.8076E-3
Mac-ADE	1.4225E-2	7.8628E-3	3.1034E-3	1.0253E-3
Mac-CN	1.4250E-2	7.8628E-3	3.1034E-3	1.0249E-3
Mac-Mac	1.4250E-2	7.8628E-3	3.1034E-3	1.0253E-3
MacCormack [27]	1.4250E-2	7.8628E-3	3.1034E-3	1.0253E-3

It can be obviously observed from Table 1 that the performance of schemes in the second class, i.e., Mac-ADE/CN/Mac is superior than the schemes in the first class, namely Upwind-ADE/CN/FTCS. In each class, the same order of accuracy is observable for all methods in the class. Form these results one immediately concludes that the performance of methods used for the discretization of convection subproblem, which has a discontinuous coefficient has a direct impact on the performance of the whole discretization method for (1.2). Indeed, the upwind-type approaches are first-order accurate while the MacCormack-type procedures are second-order. To confirm this,we take $T = 0.5$ and report the corresponding convergence rates for these methods in Table 2.

Next, for a fixed $M = 100$, we depict the numerical solutions and the exact true solutions obtained by Upwind-FTCS method at different time levels $t = \Delta t, 5\Delta t, 10\Delta t, \ldots, 45\Delta t, 50\Delta t$ in Figure 1, left. In all visualizations, the exact solutions are presented by thick lines and the numerical counterpart are depicted by (coloured) dashed lines. Furthermore, the corresponding errors in the L_1, L_2, L_∞ norms are visualized in Figure 1, right. In all plots we have used $\Delta t = 0.01$ and $\epsilon = 0.00001$.

It can be observed from Figure 1 that the numerical model results are found to be in good alignment with exact results. However, in the vicinity of discontinuities

TABLE 2. L_1 convergence rates evaluated at time $T = 0.5$ for different M based on sequential splitting for Example 3.1 with $\Delta t = 0.001$, $\epsilon = 0.001$.

M	Up [27]	Up-ADE	Up-CN	Up-FTCS	Mac-ADE	Mac-CN	Mac-Mac	Mac [27]
16	-	-	-	-	-	-	-	-
32	0.47	0.47	0.47	0.47	0.32	0.32	0.32	0.32
64	1.01	1.01	1.01	1.01	1.68	1.68	1.68	1.68
128	1.07	1.08	1.08	1.08	2.13	2.13	2.13	2.13
256	0.99	0.99	0.99	0.99	2.03	2.03	2.03	2.03
512	0.99	1.00	1.00	1.00	2.16	2.16	2.16	2.16
1024	0.99	1.01	1.00	1.02	1.52	1.99	1.99	1.99

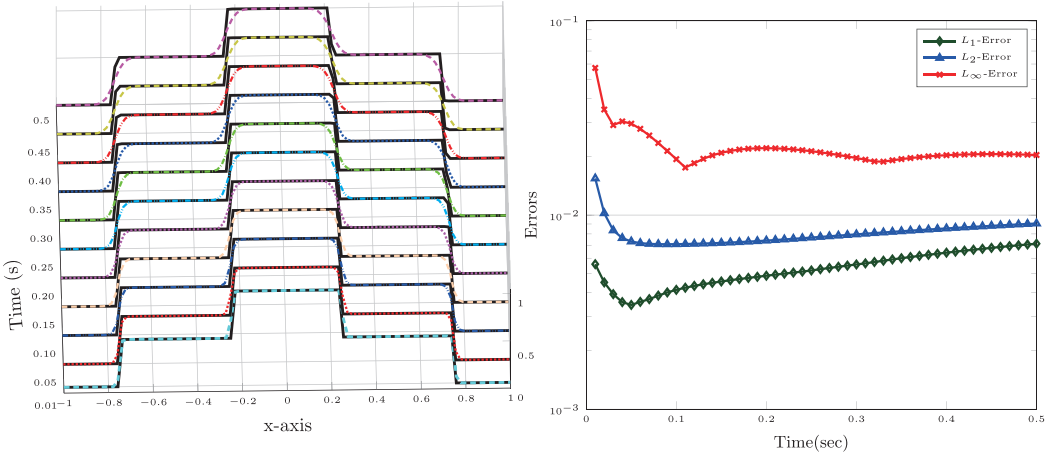

FIGURE 1. Numerical and exact solutions of Upwind-FTCS (left) and the corresponding L_1, L_2, L_∞ errors (right) of Example 3.1 at times $t = s\Delta t$ for $s = 1, 5, 10, \ldots, 46, 50\Delta t$ (left). In both cases, $M = 100$ and $\epsilon = 0.00001$.

(i.e, points $x = \pm\frac{1}{4}, \pm\frac{3}{4}$), the solutions are smeared. Note that, when ϵ is taken so small the convection term is dominated and the problem (1.2) has a hyperbolic nature than parabolic. For this example, we also utilize a second-order scheme based on the MacCormack algorithm. Under the same problem assumptions as in the Upwind-FTCS, we depict the numerical and exact solution of the scheme Mac-Mac for Example 3.1 in Figure 2, left. Also, the errors with respect to time in three different norms L_1, L_2, and L_∞ as shown in the right plot.

3.2. **Non-linear case.** To further demonstrate the accuracy of the proposed splitting finite difference schemes, we consider (1.2) with a non-linear convective flux. We take $f(u) = u^2/2$, which is known as the Burgers flux. We are aiming at solving exact solvable problems and compare the numerical results with other existing computational approaches. In the non-linear and general cases, the time step Δt

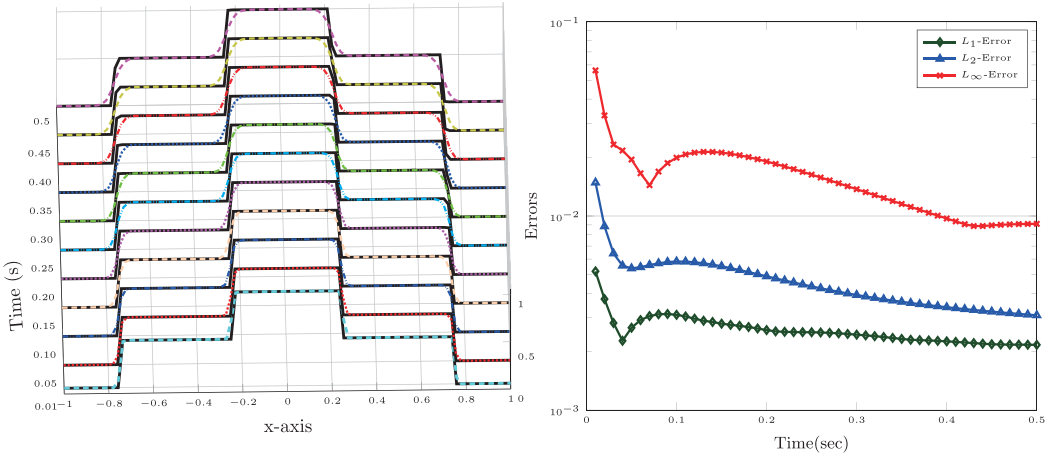

FIGURE 2. Numerical and exact solutions of Mac-Mac (left) and the corresponding L_1, L_2, L_∞ errors (right) of Example 3.1 at times $t = s\Delta t$ for $s = 1, 5, 10, \ldots, 46, 50\Delta t$ (left). In both cases, $M = 100$ and $\epsilon = 0.00001$.

should be selected so that the CFL numbers $\mu \max_{j\in\mathbb{Z}} |(f^{\pm})'(U^n_{j\pm\frac{1}{2}})| < 1$. In the computations below, we take the final time $T = 0.1$.

Example 3.2. We solve the non-linear model problem (1.2) with $\gamma^- = 0.1$ and $\gamma^+ = 0.4$ and the initial condition for this model problem is given by

$$u(x, 0) = \sin(\pi x).$$

For this problem, the viscosity is taken to be $\epsilon = 0.01$. In Table 3, as in the linear test problem we summarize the numerical errors in the L_1 norm obtained by the schemes Upwind-ADE/CN/FTCS and Mac-ADE/CN/Mac based on the sequential splitting procedure evaluated at time $T = 0.1$. All the values are obtained using $\Delta t = 0.001$ for different choices of the number of spatial grid points $M = 25, 50, 100, 200$. Although, almost the same accuracies are obtained within each upwind and MacCormack-type methods, but a slightly better result is obtained through exploiting first-order splitting procure. Moreover, Among the second-order schemes, the performance of MacCormack is also slightly better.

In the next experiment, we fix $M = 100$ and consider the scheme Mac-ADE based on the sequential splitting for Example 3.2. The numerical solutions at different time levels as a multiple of ten, i.e., after $1, 10, 20, \ldots, 90, 100$, time steps are visualized in Figure 3, left plot. We use $\Delta t = 0.001$, $\epsilon = 0.01$, and $T = 0.1$ as for the first experiments in Table 3. In all visualization, the exact solutions are shown by thick lines and the numerical counterpart are presented by (coloured) dotted, dashed, and dashed-dotted curves. In the same figure, on the right plot, the behaviour of error norms versus time in three different norms L_1, L_2 and L_∞ is represented. Looking at Fig 3 reveals that the numerical solutions obtained via Mac-ADE are in good alignment with the exact solutions.

TABLE 3. Comparison of L_1 error norms for different finite difference schemes based on sequential splitting for Example 3.2 with $\Delta t = 0.001$, $\epsilon = 0.01$, and $\Delta x = 0.08, 0.04, 0.02, 0.01$ evaluated at time $T = 0.1$.

Method	$M = 25$	$M = 50$	$M = 100$	$M = 200$
Upwind [27]	1.2754E-2	1.1595E-2	1.2306E-2	1.2481E-2
Upwind-ADE	1.1104E-2	5.6362E-3	2.7696E-3	1.3888E-3
Upwind-CN	1.1104E-2	5.6365E-3	2.7706E-3	1.4380E-3
Upwind-Mac	1.1104E-2	5.6365E-3	2.7707E-3	1.4474E-3
Mac-ADE	4.3143E-3	1.1289E-3	3.7971E-4	1.9546E-4
Mac-CN	4.3101E-3	1.1143E-3	3.9891E-4	2.7921E-4
Mac-Mac	4.3101E-3	1.1143E-3	4.0002E-4	2.9040E-4
MacCormack [27]	4.3113E-3	1.1256E-3	3.7558E-4	1.9174E-4

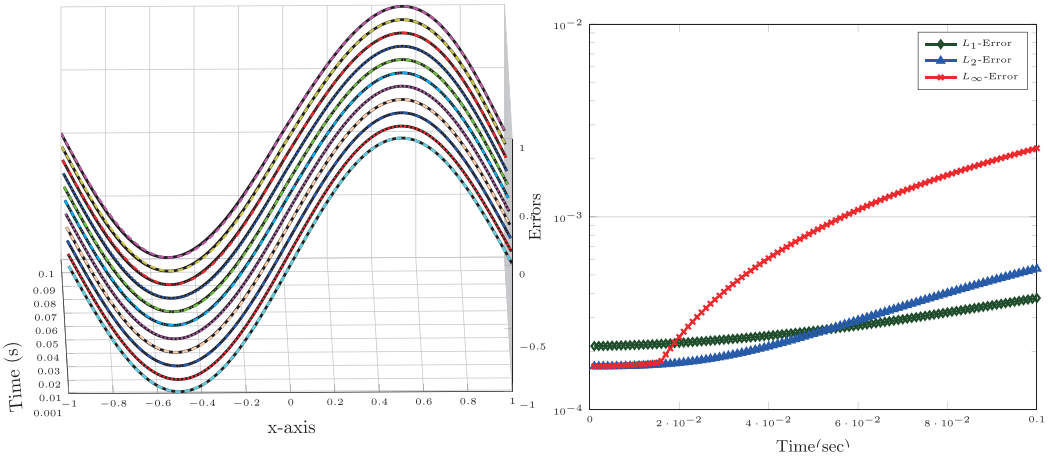

FIGURE 3. Numerical and exact solutions of Mac-ADE (left) and the corresponding L_1, L_2, L_∞ errors (right) of Example 3.2 at times $t = s\Delta t$ for $s = 1, 10, 20 \ldots, 90, 100\Delta t$ (left). In both cases, $M = 100$ and $\epsilon = 0.01$.

4. CONCLUSIONS

A class of finite-difference algorithms based on operator splitting has been developed for the (non-linear) convection-diffusion problems having discontinuous coefficient arising from modelling many real-world phenomena. While the convective subproblem is discretized by the first-order upwind and second-order MacCormack procedures, the diffusion subproblem is solved by means of three popular unconditionally stable finite difference methods. We have compared both the first and second-order methods using explicit codes, in both linear and non-linear test problems. The discussed computational procedures solved our model quite satisfactorily compared to the existing and standard finite difference algorithms.

Our computational experiments for (1.2) show that the accuracy of the whole splitting procedures is restricted on the accuracy of the methods applied to the convection subproblem (2.2a) that has a discontinuous coefficient. While there are many high-order accurate schemes available in literature for the diffusion subproblem (2.2b), finding such methods for (2.2a) is not a straightforward task. Therefore, the first attempt in this direction is to devise higher-order methods for (2.2a). Generalizations of these methods to higher dimensions are also of interest and needs further investigations.

References

[1] H. Z. Barakat and J. A. Clark, *On the solution of the diffusion equations by numerical methods*, Trans. ASME J. Heat Transfer **88** (1966), 421–427.

[2] R. Bürger, K. H. Karlsen, N. H. Risebro and J. D. Towers, *Numerical methods for the simulation of continuous sedimentation in ideal clarifier-thickener units*, Internat. J. Miner. Process. **73** (2004), 209–228.

[3] D. Chouhan, V. Mishra and H. M. Srivastava, *Bernoulli wavelet method for numerical solution of anomalous infiltration and diffusion modeling by nonlinear fractional differential equations of variable order*, Results Appl. Math. **10** (2021): Article ID 100146.

[4] M. Crandall and A. Majda, *The method of fractional steps for conservation laws*, Numer. Math. **34** (1980), 285–314.

[5] S. Diehl, *On scalar conservation laws with point source and discontinuous flux function*, SIAM J. Math. Anal. **26** (1995), 1425–1451.

[6] S. Diehl, *A conservation law with point source and discontinuous flux function modelling continuous sedimentation*, SIAM J. Appl. Math. **56** (1996), 388–419.

[7] T. Gimse and N. H. Risebro, *Solution of the Cauchy problem for a conservation law with a discontinuous flux function*, SIAM J. Math. Anal. **23** (1992), 635–648.

[8] S. K. Godunov, *Finite difference methods for numerical computations of discontinuous solutions of the equations of fluid dynamics*, Mat. Sb. **47** (1959), 271–306 (in Russian).

[9] H. Holden and N. H. Risebro, *A mathematical model of traffic flow on a network of unidirectional roads*, SIAM J. Math. Anal. **26** (1995), 999–1017.

[10] M. Izadi,*Streamline diffusion method for treating coupling equations of hyperbolic scalar conservation laws*, Math. Comput. Model. **45** (2007), 201–214.

[11] M. Izadi, *A posteriori error estimates for the coupling equations of scalar conservation laws*, BIT Numer. Math. **49** (2009), 697–720.

[12] M. Izadi, *Application of the Newton-Raphson method in a SDFEM for inviscid Burgers equation*, Comput. Methods Differ. Equ. **8** (2020), 708–732.

[13] M. Izadi, *Split-step finite difference schemes for solving the nonlinear Fisher equation*, J. Mahani Math. Res. Cent. **7** (2018), 37–55.

[14] M. Izadi, *A second-order accurate finite-difference scheme for the classical Fisher-Kolmogorov-Petrovsky-Piscounov equation*, J. Inform. Optim. Sci. **42** (2021), 431–448.

[15] *M. Izadi, Two-stages explicit schemes based numerical approximations of convection-diffusion equations*, Internat. J. Comput. Sci. Math. **15** (2022), in press.

[16] M. Izadi and H. M. Srivastava, *An optimized second order numerical scheme applied to the non-linear Fisher' s reaction-diffusion equation*, J. Interdisciplinary Math. **25** (2022), 471–492.

[17] K. H. Karlsen and N. H. Risebro, *An operator splitting method for nonlinear convection-diffusion equations*, Numer. Math. **77** (1997), 365–382.

[18] K. H. Karlsen, N. H. Risebro and J. D. Towers, *Upwind difference approximations for degenerate parabolic convection-diffusion equations with a discontinuous coefficient*, IMA J. Numer. Anal. **22** (2002), 623–664.

[19] K. H. Karlsen, N. H. Risebro and J. D. Towers, L^1 *stability for entropy solutions of nonlinear degenerate parabolic convective-diffusion equations with discontinuous coefficients*, Skr. K. Vidensk. Selsk. **3** (2003), 1–49.

[20] T. Jahnke and C. Lubich, *Error bounds for exponential operator splittings*, BIT Numer. Math. **40** (2000), 735–744.
[21] R. J. LeVeque, *Numerical Methods for Conservation Laws*, Birkhauser-Verlag, 1992.
[22] R.W. MacCormack, The effect of viscosity in hypervelocity impact cratering, J. Spacecr. Rockets. **40**(5) (2003), 757–763.
[23] S. Mochon, *An analysis of the traffic on highways with changing surface conditions*, Math. Model. **9** (1987), 1–11.
[24] L. Mahto, S. Abbas, M. Hafayed and H. M. Srivastava, *Approximate controllability of sub-diffusion equation with impulsive condition*, Mathematics **7** (2019), Article ID 190.
[25] N. Okhovati and M. Izadi, *Numerical coupling of two scalar conservation laws by a RKDG method*, J. Korean Soc. Industr. Appl. Math. **23** (2019), 211–236.
[26] N. Okhovati and M. Izadi, *A predictor-corrector scheme for conservation equations with discontinuous coefficients*, J. Math. Fund. Sci. **52** (2020), 312–327.
[27] V. K. Saul'yev, *A method of numerical solution for the diffusion equations*, Dokl. Akad. Nauk SSSR **115** (1957), 1077–1099 (in Russian).
[28] V. K. Saul'yev, *Integration of Equations of Parabolic Type by the Method of Nets*, Pergamon Press, Oxford, 1964.
[29] H. M. Srivastava, H. Ahmad, I. Ahmad, P. Thounthong and M. N. Khan, *Numerical simulation of 3-D fractional-order convection-diffusion PDE by a local meshless method*, Thermal Sci. **25** (2021), 347–358.
[30] H. M. Srivastava and M. Izadi, *The Rothe-Newton approach to simulate the variable coefficient convection-diffusion equations*, J. Mahani Math. Res. Cent. **11** (2022), 141–147.
[31] G. Strang, *On the construction and comparison of different splitting schemes*, SIAM. J. Numer. Anal. **5** (1968), 506–517.
[32] A. Tassaddiq, M. Yaseen, A. Yousaf and R. Srivastava, *A cubic B-spline collocation method with new approximation for the numerical treatment of the heat equation with classical and non-classical boundary conditions*, Physica Scripta **96** (2021): Article ID 045212.
[33] J. W. Thomas, *Numerical Partial Differential Equations*: *Finite Difference Methods*, Springer, Berlin, Heidelbergh and New York, 1995.
[34] X. Wen and S. Jin, *Convergence of an immersed interface upwind scheme for linear advection equations with piecewise constant coefficients I: L_1-error estimates*, J. Comput. Math. **26** (2008), 1–22.
[35] X.-J. Yang, J. A. T. Machado and H. M. Srivastava, *A new numerical technique for solving the local fractional diffusion equation: Two-dimensional extended differential transform approach*, Appl. Math. Comput. **274** (2016), 143–151.
[36] X.-J. Yang, H. M. Srivastava, D. F. M. Torres and A. Debbouche, *General fractional-order anomalous diffusion with non-singular power-law kernel*, Thermal Sci. **21** (Suppl. 1) (2017), S1–S9.
[37] K. V. Zhukovsky and H. M. Srivastava, *Analytical solutions for heat diffusion beyond Fourier law*, Appl. Math. Comput. **293** (2017), 423–437.

Manuscript received May 18 2022
revised June 19 2022

H. M. Srivastava
Department of Mathematics and Statistics, University of Victoria, Victoria, British Columbia V8W 3R4, Canada;
Department of Medical Research, China Medical University Hospital, China Medical University, Taichung 40402, Taiwan, Republic of China;
Department of Mathematics and Informatics, Azerbaijan University
71 Jeyhun Hajibeyli Street, AZ1007 Baku, Azerbaijan;
Section of Mathematics, International Telematic University Uninettuno, I-00186 Rome, Italy
E-mail address: harimsri@math.uvic.ca

M. Izadi
Department of Applied Mathematics, Faculty of Mathematics and Computer, Shahid Bahonar University of Kerman, Kerman 76169-14111, Iran
E-mail address: izadi@uk.ac.ir

N. Okhovati
Department of Mathematics, Kerman Branch, Islamic Azad Uiversity, Kerman 76169-14111, Iran
E-mail address: diamand_2010@yahoo.com